

# Electronic Structure of Elongated $\text{In}_{0.3}\text{Ga}_{0.7}\text{As}/\text{GaAs}$ Quantum Dots

M. PIECZARKA\*, A. MUSIAŁ, P. PODEMSKI, G. SEK AND J. MISIEWICZ

Institute of Physics, Wrocław University of Technology, Wybrzeże Wyspiańskiego 27, 50-370 Wrocław, Poland

In this contribution the electronic structure of large  $\text{In}_{0.3}\text{Ga}_{0.7}\text{As}/\text{GaAs}$  quantum dots is studied theoretically by means of 8 band  $\mathbf{k} \cdot \mathbf{p}$  modeling. These quantum dots constitute unique physical system due to the low strain limit of the Stranski–Krastanow growth mode resulting in relatively large physical volume and elongation of the quantum dots in [1–10] direction. As a result of these critical growth conditions the electronic structure is expected to be very sensitive to the nanostructure size, shape, and composition of the quantum dot as well as the accompanying wetting layer. Another peculiarity of investigated system is the confining potential which is rather shallow and weakened in comparison to standard quantum dots. It makes them very interesting in view of both fundamental study and potential applications. To reveal physical mechanisms determining the optical properties of the investigated system, the electronic structure, mainly the number of confined states, and the wave function extension as a function of both quantum dot size and geometry have been simulated numerically and the importance of electron–hole Coulomb interactions has been evaluated.

DOI: [10.12693/APhysPolA.124.809](https://doi.org/10.12693/APhysPolA.124.809)

PACS: 78.67.Hc, 73.21.La, 73.22.–f

## 1. Introduction

Tremendous development in epitaxial growth techniques allowed the formation of zero-dimensional semiconductor nanostructures, which have opened up unprecedented opportunities for tuneability of the physical properties and have been proven beneficial first for optoelectronic applications [1, 2] and further for more advanced single quantum dot-based photonic devices. The electronic structure and resulting optical properties of quantum dots (QDs) in a given material system can be tuned via QD shape, geometry as well as composition distribution which, on the other hand, are determined by the growth conditions. Controllable design of nanostructures fulfilling practical requirements is highly desired and has to be supported by the fundamental study of interdependence between the structural and optical properties.

As far as QD-based emitters are considered, very important issue is to maximize the oscillator strength of optical transitions, which determines the efficiency of the source as well as the response time of QD-based devices. One of the approaches to achieve this goal is to increase the physical volume of the nanoobject and reach the weak confinement regime, in which the oscillator strength increases with the exciton coherence volume as it has been observed and argued for natural quantum dots [3, 4]. Large  $\text{In}_{0.3}\text{Ga}_{0.7}\text{As}/\text{GaAs}$  nanostructures are an example of realization of this idea for epitaxial QDs.

Increased physical volume has been obtained by decreasing the strain during growth employing low indium (30%)  $\text{InGaAs}$  alloy compound and reducing the lattice

mismatch with GaAs substrate down to 2% [5]. This enabled to achieve the first realization of strong coupling between the single exciton and single photon in the micropillar cavity [6].

This work aims at modeling the electronic structure of such QDs and focuses on the number and separation of confined levels for various QD sizes and geometries to determine the conditions for strictly QD-related transitions in the case of shallow confining potential. These have not yet been analyzed in the literature. The wave function extension in the single particle picture has been confronted with the outcome of the calculations including excitonic corrections in the Hartree approximation. The presented numerical simulations have been performed within the 8 band  $\mathbf{k} \cdot \mathbf{p}$  model using the *nextnano++* software [7].

## 2. The model

To determine the electronic structure of a QD system the 8 band  $\mathbf{k} \cdot \mathbf{p}$  model has been utilized. The three-dimensional strain distribution has been calculated in the continuum elasticity model including the first order piezoelectric effect. The Coulomb correlations have been added in the Hartree approximation, in which the excitonic correction (resulting from the electron–hole Coulomb attraction) has been calculated and the single particle wave functions have been modified accordingly. Material parameters used in the modeling are taken after [8].

All numerical simulations have been performed for  $\text{InGaAs}/\text{GaAs}$  QDs with nominal indium content of 30% and homogeneous indium distribution. Interfaces between the adjacent layers were described as ideal. Semielliptical (lens-shape) geometry of the quantum dots was assumed and the dimensions were varied in the range of

\*corresponding author; e-mail: [maciej.pieczarka@pwr.wroc.pl](mailto:maciej.pieczarka@pwr.wroc.pl)

40–100 nm, 20–40 nm and 3–4 nm for QD length, width and height, respectively, realistic for such QD structures [5]. The quantum dot was placed on the 2.7 nm thick wetting layer (WL) quantum well (after [9]) and oriented so that the elongation direction coincides with the [1–10] crystallographic direction, as in the real structure. In content distribution was assumed as constant and 30% both in the dot and the WL. The active region was surrounded by the GaAs material. The interfaces between two different semiconductors were assumed as ideal.

### 3. Results and discussion

At first, the depth of confining potential has been examined for different QD sizes and geometries and the number of confined states and their separation has been determined. The calculations were performed in a standard approach, in which the discrete  $\mathbf{k} \cdot \mathbf{p}$  Hamiltonian is diagonalized and the Poisson equation is solved self-consistently. As a result, the confining potential for electrons and holes together with the eigenstates of the system are obtained. Subsequently, the confined states have been identified using two criteria i.e., energetic (the eigenenergy below the 2D continuum of states of the ideal WL) and spatial one (the maximum of the probability distribution of the eigenstate is localized geometrically in the QD).

The example of the confining potential profile at the  $\Gamma$  point along the growth direction through the centre of the dot for a typical QD geometry of  $80 \times 40 \times 4 \text{ nm}^3$  is presented in Fig. 1. The localization energy (the difference between the confined state energy and the edge of the 2D continuum of states in the WL) of carriers confined within the QD calculated in the single particle picture is rather small with respect to the WL, i.e. approximately 50 meV for electrons (el) and in the single meV range for holes (hh). These values are of the same order as activation energies obtained experimentally on the basis of the Arrhenius analysis of photoluminescence quenching [10]. Lower values obtained in the experiment (25–35 meV) can be a result of differences in the assumed and actual QD geometry, together with its variation within the QD ensemble.

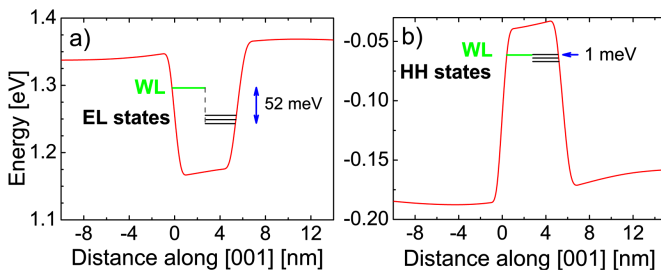


Fig. 1. Conduction (a) and valence (b) band profiles at  $\Gamma$  point along the growth direction through the centre of the dot, together with the lowest electron and hole energy states.

As a result of this shallow confining potential the number of states confined in the QD is very limited, especially if the hole states are considered. In the presented example (Fig. 1) heavy hole-like states are energetically very close to the 2D continuum of states of the ideal WL and even though only one of them is above this energy, the potential confines the hole probability density distribution spatially still mainly within the QD volume, preserving significant overlap with the electron states, even though its leakage into the WL/barrier region is not negligible.

For the largest QDs with 80 and 100 nm lengths and height in the range of 3–4 nm there are two or even three strong optical transitions between the electron and hole states confined within the QD (Fig. 2) and the energy splitting of the transitions between the lowest el and hh states and the first excited ones (in symmetrical structures denoted as an  $s$ - $p$  shell splitting) is in the range of 10 meV, smaller than the values observed in microphotoluminescence ( $\mu$ PL) experiments [11] which suggests either that the QDs are typically much smaller than 80 nm in the elongation direction, or that assumed In content or distribution is far from realistic. More complicated In distributions have been reported for InGaAs QDs [12, 13] due to indium tendency to segregation, but examination of these effects is beyond the scope of this paper.

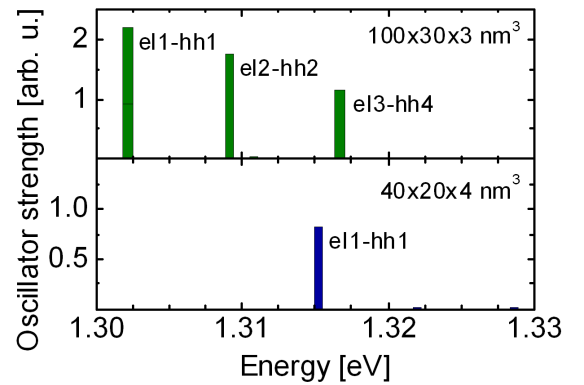


Fig. 2. Energetic structure and oscillator strengths for optical transitions between the states confined in the QD with the strongest electron-hole wave function overlap integral, el1-hh1, el2-hh2, el3-hh4, respectively for QD:  $100 \times 30 \times 3 \text{ nm}^3$  (upper part) and for QD:  $40 \times 20 \times 4 \text{ nm}^3$  (lower part).

Generally, indium aggregation towards the top of the quantum dot should provide stronger quantum confinement due to the increased contrast of the WL/QD composition which can be a reason of underestimated splitting of the fundamental and excited states transitions obtained in our simulations. On the other hand, the excited state energy of the QDs can coincide with the WL emission energy range and, due to the localized character of the lowest wetting layer states [14, 15] in such structures, it is not that straightforward to distinguish between the QD-like and WL-related emission in this spectral range in the case of  $\mu$ PL measurements.

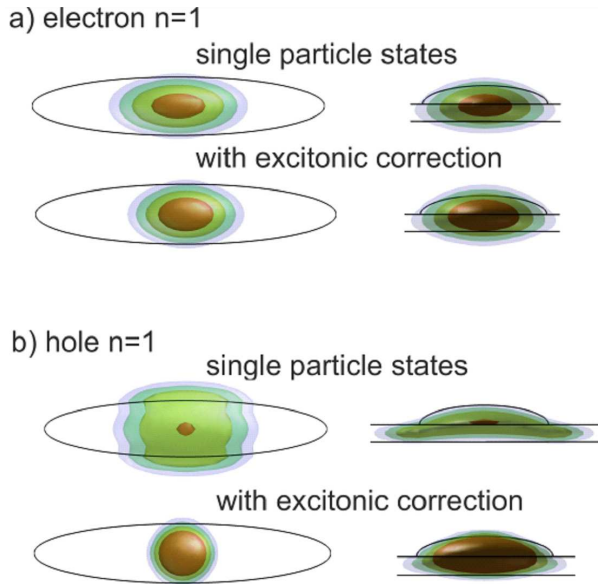


Fig. 3. Electron (a) and hole (b) isosurface 3D plots of the probability density distribution  $P$  (color scale:  $P = 0.4, 0.2, 0.1, 0.05$ , respectively): top view (left column) and cross-section in  $[110]$  direction (right column) in the single particle picture (top row) and with excitonic correction included in Hartree approximation (bottom row) for  $100 \times 20 \times 4 \text{ nm}^3$  QD.

When the absolute emission energy of the modeled QDs is compared with the experimentally obtained maximum of the ensemble emission band [9], the corresponding relevant QD geometry should be close to  $40 \times 20 \times 4 \text{ nm}^3$ , but for such structural parameters only one optical transition related with the QDs can be observed (Fig. 2). Also the confining potential, and as a result the electronic structure is rather sensitive to variation in the QD geometry. This can be attributed to changes in the strain distribution and following piezoelectric effect influencing the band edges of the confining potential. Furthermore, the strain-induced band edge deformation leads to larger ground state transition energy for higher QDs with exactly the same remaining dimensions (results not presented here) in contrast to the typically observed size effect, i.e. decreasing energy of the confined states with increasing 1D potential well width.

The pointed out discrepancies with the experimental results might be related to the significantly weakened quantum confinement expected due to the relatively large nanostructure physical volume as compared to the exciton coherence volume defined by the exciton Bohr radius (in the range of 19 nm for  $\text{In}_{0.3}\text{Ga}_{0.7}\text{As}$  alloy compound [16]). In such conditions the single particle picture is not relevant anymore and the Coulomb correlations need to be included. This is realized in the Hartree approximation and the respective results are presented below.

The excitonic correction has been calculated and now the modification of single particle wave functions for rep-

resentative QD geometry ( $100 \times 20 \times 4 \text{ nm}^3$ ) will be discussed (Fig. 3). As can be seen in Fig. 3a the excitonic effects do not influence the electron ground state probability distribution strongly, i.e. they increase slightly the in-plane symmetry and simultaneously provide extension of the highest distribution probability region. The former is beneficial for polarization insensitive gain as well as unpolarized surface emission and small exciton fine structure splitting required for photon indistinguishability. The latter can be one of the reasons of light-matter interaction enhancement observed experimentally [6]. This proves that the electron states are not strongly affected by the Coulomb interactions as they are already confined within the QD.

The picture is completely different for hole states which wave function (probability density) is leaking into the WL/barrier and the probability density distribution is smeared out over the volume larger than the physical volume of the QD. When the excitonic correction is included, the probability distribution changes dramatically, i.e. it becomes almost symmetrical in-plane and confined within the QD as the leakage to the WL/barrier is strongly reduced. These changes and their consequences are similar to those previously discussed for electrons, but the effect is critical for holes as they are very weakly localized in the quantum dot. The importance of the Coulomb correlations on the electronic structure can be traced back to the weakened confinement regime indicated indirectly in [14].

The modification of the carrier probability distribution can account for the experimental observations. The emission energy of the ground state will be red shifted by the exciton binding energy which has been calculated to be in the range of 13–16 meV depending on the exact QD geometry. With such excitonic correction, the comparison between the calculated and observed experimentally ground state transition energy suggests larger typical size of a QD than indicated previously based on the single particle calculations. As a result, carriers experience deeper confining potential. Abovementioned observations show that the single particle picture is inadequate to describe electronic structure of large  $\text{In}_{0.3}\text{Ga}_{0.7}\text{As}/\text{GaAs}$  quantum dots and the optical properties of emission are in this case governed primarily by the excitonic effects making the exact QD geometry less important.

#### 4. Conclusions

In conclusion, the electronic structure has been described and its driving factors have been identified using 8 band  $\mathbf{k} \cdot \mathbf{p}$  approach. Due to the critical low strain growth conditions, on the verge of the Stranski-Krastanow mode, the electronic structure of confined states is extremely sensitive to the QD size and geometry. The structural parameters enabling electron and hole localization within the QD have been found, but even though the shallow confining potential for hole states results in the wave function leakage to the barrier and/or

WL. The crucial modification of the hole probability density distribution introduced by the excitonic effects proves the weak quantum confinement regime as indicated in the experiments. The wave function becomes in general rather symmetric in spite of QD elongation which should be reflected in the lowered anisotropy of optical properties of emission, especially in the polarization of emitted radiation, which in that case will be governed neither by the QD shape nor the confining potential anisotropy.

### Acknowledgments

The authors acknowledge the financial support from the Foundation for Polish Science (FNP) and Deutsche Forschungsgemeinschaft (DFG) — COPERNICUS Award and the National Science Centre of Poland within grant MAESTRO No. 2011/02/A/ST3/00152.

### References

- [1] Y. Arakawa, H. Sakaki, *Appl. Phys. Lett.* **40**, 939 (1982).
- [2] *Nano-Optoelectronics: Concepts, Physics and Devices*, Ed. M. Grundmann, Springer, Berlin 2002.
- [3] L.C. Andreani, G. Panzarini, J.M. Gerard, *Phys. Rev. B* **60**, 13276 (1999).
- [4] M. Wimmer, S.V. Nair, J. Shumway, *Phys. Rev. B* **73**, 165305 (2006).
- [5] A. Löffler, J.P. Reithmaier, A. Forchel, A. Sauerwald, D. Peskes, T. Kümmell, G. Bacher, *J. Cryst. Growth* **286**, 6 (2006).
- [6] J.P. Reithmaier, G. Sęk, A. Löffler, C. Hofmann, S. Kuhn, S. Reitzenstein, L. Keldysh, V. Kulakovskii, T. Reinecke, A. Forchel, *Nature* **432**, 197 (2004).
- [7] More about the software at: [www.nextnano.de](http://www.nextnano.de).
- [8] I. Vurgaftman, J.R. Meyer, L.R. Ram-Mohan, *J. Appl. Phys.* **89**, 5815 (2001).
- [9] P. Poloczek, G. Sęk, J. Misiewicz, A. Löffler, J.P. Reithmaier, A. Forchel, *J. Appl. Phys.* **100**, 013503 (2006).
- [10] A. Musiał, G. Sęk, A. Maryński, P. Podemski, J. Misiewicz, A. Löffler, S. Höfling, S. Reitzenstein, J.P. Reithmaier, A. Forchel, *Acta Phys. Pol. A* **120**, 883 (2011).
- [11] S. Reitzenstein, S. Münch, P. Franeck, A. Rahimi-Iman, A. Löffler, S. Höfling, L. Worschech, A. Forchel, *Phys. Rev. Lett.* **103**, 127401 (2009).
- [12] T. Walther, A.G. Cullis, D.J. Norris, M. Hopkinson, *Phys. Rev. Lett.* **86**, 2381 (2001).
- [13] N. Liu, J. Tersoff, O. Baklenov, A.L. Holmes, Jr., C.K. Shih, *Phys. Rev. Lett.* **84**, 334 (2000).
- [14] G. Sęk, A. Musiał, P. Podemski, M. Syperek, J. Misiewicz, A. Löffler, S. Höfling, L. Worschech, A. Forchel, *J. Appl. Phys.* **107**, 096106 (2010).
- [15] M. Syperek, M. Baranowski, G. Sęk, J. Misiewicz, A. Löffler, S. Höfling, S. Reitzenstein, M. Kamp, A. Forchel, *Phys. Rev. B* **87**, 125305 (2013).
- [16] *Handbook on Physical Properties of Semiconductors*, Vol. 2, *III-V Compound Semiconductors*, Ed. S. Adachi, Springer, Boston 2004.